THE GEOMAGNETICALLY TRAPPED RADIATION ENVIRONMENT

---A RADIOLOGICAL POINT OF VIEW---

F. Eugene Holly, Ph.D.
Air Force Weapons Laboratory
Kirtland AFB, New Mexico

The regions of naturally occurring, geomagnetically trapped radiation (Van Allen Belts) are briefly reviewed in terms of physical parameters such as; particle types, fluxes, spectrums, and spatial distributions. The major emphasis is, however, placed upon a description of this environment in terms of the radiobiologically relevant parameters of absorbed dose and dose-rate and a discussion of the radiological implications in terms of the possible impact on space vehicle design and mission planning.

These descriptions are based both upon direct measurement and calculation using the more fundamental parameters of particulate energy and flux. Comparison of such calculations with measurements emphasizes that, depending upon the location in space, that calculational techniques are extremely dependent upon detailed knowledge of either the energy spectrum or material (shielding) distribution about the dose point -- or both.

INTRODUCTION

Since Van Allen's (ref. 1) discovery of areas of geomagnetically trapped radiation in 1958, there has been a tremendous amount of attention focused upon this phenomena. Upon only a cursory examination of launch records (refs. 2-5), it is easy to identify over a hundred satellites and several times that many non-orbital vehicles, during the 10 year period 1958-1968, which contained radiation measuring instrumentation. These experimental packages ranged from emulsions and simple/geiger systems, with which the discovery of the belts and the first identifications of electrons and protons were made (refs. 1, 6, 7), to extreme complexity. Some satellites carried several dozen different experiments. Many excellent reviews concerning the trapped radiation environment have been written (refs. 2, 8-16). White's (ref. 8) is perhaps the most succinct and easily read, while those interested in a rigorous treatment may consult Hess (ref. 2). Reference 16 is a compilation of all experimental data dealing with radiological parameters.

PHYSICAL PARAMETERS

Largely due to the efforts of Vette (refs. 17, 18), the results of a large number of satellite experiments have been combined to form a model of the geomagnetically trapped radiation zones. These environmental models are available in the form of synoptic maps of flux and energy spectrums (refs. 12, 16, 17, 18, 19, 20) and use the systematic coordinates B and L or R and λ, which were developed by McIllwain (ref. 21). B is the magnetic field strength and L is a "magnetic shell" parameter relating the distance from the center of the earth through the magnetic equator to the point of interest. R is related to L through the expression $R = L\cos^2\lambda$, and λ is the angle to the geomagnetic equator. R and λ are not the same as the geographic altitude and latitude and can be obtained only from the B-L system. For further discussions of these coordinate systems, the reader is referred to reference 21 and Chapter II of reference 16.

In general, the parameters which are of interest to designers and planners are those which will cause detectible influence on man or machine and these will be given the more thorough scrutiny by this writing.

Protons: There are distributions of high energy (10 to many hundred MeV) protons whose intensity varies with spatial location and has a maximum intensity at about L = 1.5 (L is expressed in units of earth radii). The intensity decreases to about 10^{-3} to 10^{-4} of maximum intensity at L = 3.0 with a smaller secondary maximum occuring at L = 2.2. At the position of the primary maximum, the integral flux above 34 MeV is approximately 2×10^{4} cm $^{-2}$ sec^{-1}. The spectral shape, although dependent upon spatial location, generally may be represented as decreasing exponentially, as shown in Figure 1 (ref. 16). Secondly, there are multilayers of low energy protons (0.1 to 10 MeV) surrounding the earth like "concentric skins on an onion" (ref. 8) with increasing energy toward the earth.

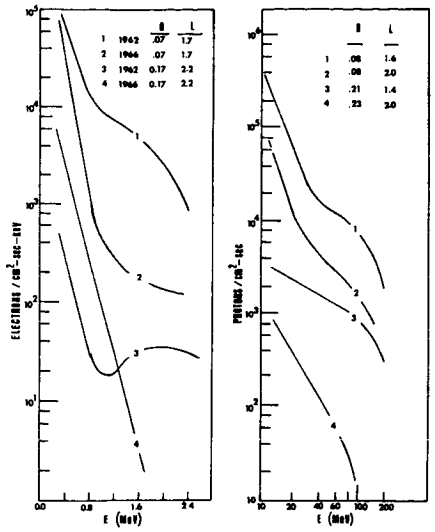

1. Typical trapped electron and proton spectrums. The difference in hardness of the 1962 and 1966 spectrums is due to the decay or loss of the artificially injected Starfish fission-electrons.

Electrons: There are two intense electron belts widely separated by a "slot" of considerably less and varying intensity. The "inner belt" maximum intensity occurs at L = 1.4 and has an integrated intensity above 0.5 MeV greater than 10^8 cm^{-2} sec^{-1} and consists of electrons with energies from a few keV to several MeV. This region is made up, primarily, of artificially injected electrons from the Starfish high-altitude nuclear explosion (1962) and does not fluctuate; however, the intensity decreases slowly with time as the electrons are lost into the atmosphere. The "outer belt", extending from L = 3 to L = 6, consists of natural electrons of lower energies and fluctuates with time. The integrated intensity above 0.5 MeV, at the maximum of this belt (L = 4.5 to L = 5), is in excess of 10^6 $cm^{-2}sec^{-1}$. Although there were no extensive spectral measurements prior to the Starfish event, the inner belt electrons were identified in 1959, and the differential energy spectrum measured at L = 1.3, B = 0.25 (ref. 7). This spectrum decreased by a factor of 20 over the energy range from 100 to 450 keV and less than 3% of the measured electrons could have had energies in excess of 1 MeV. Cladis, et. al., (ref. 22) found that, in 1960, the outer belt could essentially be characterized exponentially with a 60 keV e-folding between 50 and 700 keV, a much steeper spectrum than the inner belt. These pre-Starfish spectrums may be compared with the 1962 (ref. 23) and 1966 (ref.24) spectral determinations shown in Figure 1, which include the Starfish electrons. Qualitatively, one may conjecture that the soft component shown is natural and that the harder component is the artificial contribution.

Heavy Ions: Krimigis and Van Allen (ref.25), in 1967, first established the presence of heavy ions (helium nucleii) trapped in the geomagnetic field out to distances of 4 earth radii. The energy spectra are not unlike exponential functions and their intensity varies from 0.1 to 10% of the trapped proton component, depending upon spatial location. If, however, the intensities of both components are integrated above a common 0.5 MeV/nucleon energy, the helium to proton flux ratio is approximately 2 x 10^{-4} at L = 3.1, B = 0.19.

A composite pictorial representation of the more penetrating components of the trapped environment is shown in Figure 2. The distributions of electrons with energies in excess of 0.5 MeV are displayed on the right side of the figure and proton distributions with energies exceeding 34 MeV are shown on the left. These distributions, of course, are contours of revolution around the earth and neither the many layers of low energy protons nor the heavy nucleii are represented.

RADIOLOGICAL PARAMETERS

The mission planner or spacecraft designer, who must determine potential material damage or biological hazards, is concerned with the energy that is deposited per unit volume at points of interest which are usually located within hetrogeneous shield configurations. In such cases, an expression of absorbed dose at the point of interest is a highly useful parameter. This necessitates transport through surrounding shielding and calculation of energy deposition at a specific location. The trapped radiation environment with particle types, fluxes, and energy spectrums changing kaleidoscopically with spatial position (not to mention time) poses an extremely onerous task. This is further compounded, in the case of calculation of biological hazards, where the critical location may be influenced by spectral shape (i.e., a steep spectrum is more likely to reach an internal organ, with a low tolerance, than a soft spectrum). If the physical parameters are known in sufficient detail, these tasks may be accomplished with the aid of sophisticated computer programs; however, it is expensive and time consuming. In cases where the dose or dose-rate is needed only at selected points in space or the determination of only maximum levels is necessary, an environmental model expressed in terms of absorbed dose or dose-rate is the most practical tool. Such a model, including shield thickness as a parameter, obviates the necessity for lengthy computer calculations except where complex orbital parameters are involved or where extreme accuracy is required.

Contributions in this area have been made by the Biophysics Division of the Air Force Weapons Laboratory (ref. 16). Between July 1961 and May 1969, thirteen satellites and two suborbital probes were instrumented with combinations of instrumentation for the simultaneous measurement of both radiological and physical parameters. The dosimetric instrumentation consisted of tissue-equivalent ionization chambers, which responded with better than 90% accuracy (in mixed gamma, electron, and proton fields) from a few mr/hr to several hundred r/hr and advanced devices for the measurement of linear-energy-transfer (LET) in small volumes (refs. 16, 26, 27, 28, 29). These instruments were surrounded with varying amounts of either tissue-equivalent or elemental shields. The OV1-2 and OV3-4 satellites were typical of these vehicles and were designed for two specific purposes: (1) to provide a comprehensive synoptic dose-rate map of the trapped

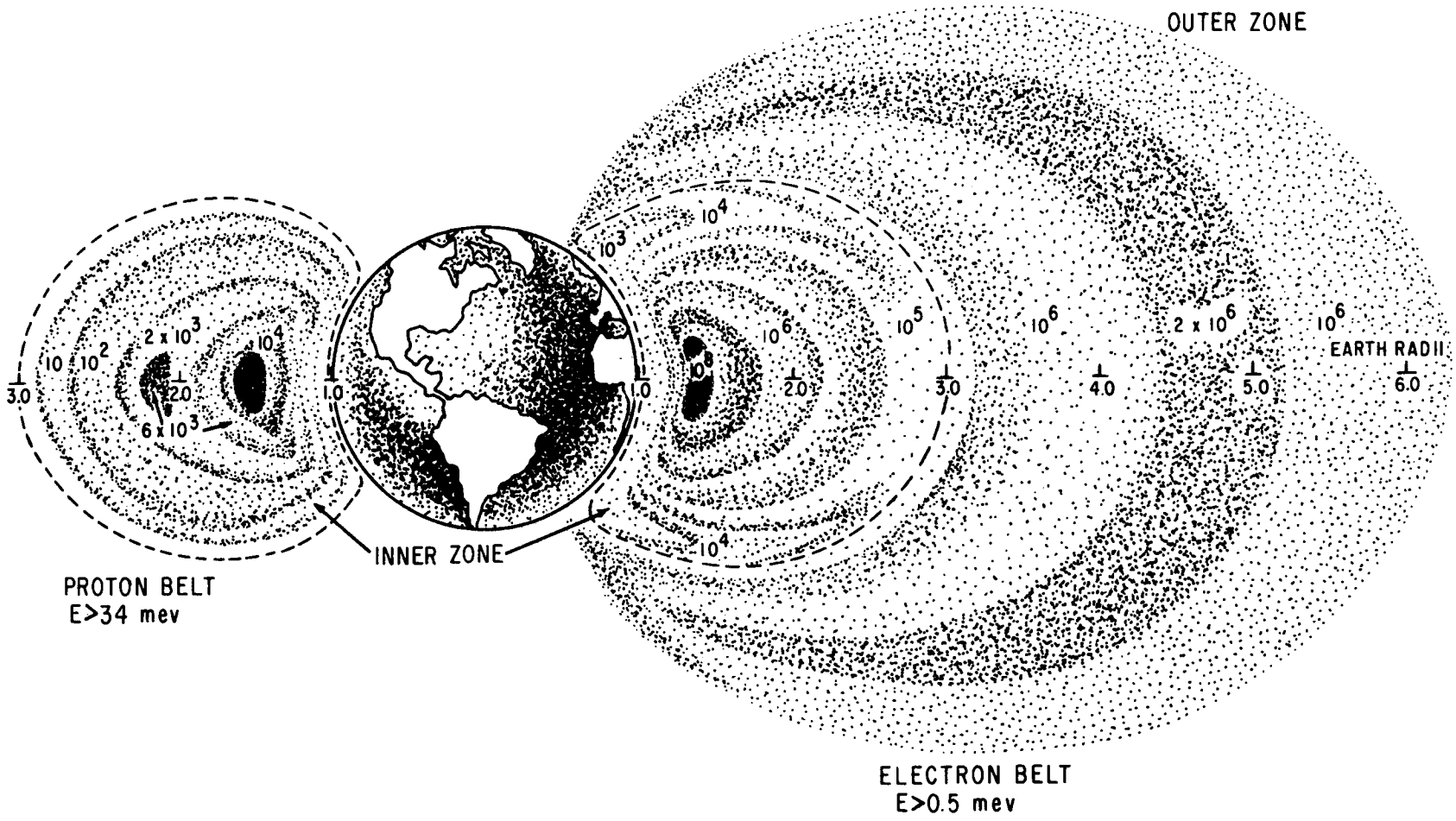

TRAPPED RADIATION ZONES

Figure 2. A model of the penetrating components of the trapped radiation environment, showing electrons on the right and protons on the left.

environment and (2) to study the effects of radiation spectra, anisotropy, and shielding hetrogeneity on the calculation of electron, proton, and bremsstrahlung doses (refs. 16, 30, 31, 32). The instrument complements of these satellites is shown in Tables 1 and 2. In addition, further data was obtained by active and passive dosimetry systems flown in a number of Gemini and Apollo missions (refs. 16, 33, 34).

Dose-rate maps based on data from four of these satellites and the Gemini flights have recently been made available by reference 16. These are in either the B, L isodose format of Figure 3; the Dose-rate, B, Iso-L format of Figure 4; or geographic projections of isodose contours at different altitudes. These are plotted in terms of dose rate beneath shielding material or in a more universally usable form of thickness of aluminum equivalent material. Table 3 gives a concise summary of the maps which are available in terms of B, L, dose-rate, and and shielding thickness ranges. Data reduction efforts currently being performed will result in the production of comprehensive synoptic dose-rate maps covering the following ranges of parameters: (1) L = 1 - 5 earth radii, (2) B = .05-0.36 gauss, and (3) 0 - 16 gm/cm aluminum equivalent thickness of shielding material (ref. 35).

TABLE 1

TYPICAL INSTRUMENTATION FOR MEASUREMENT
of
PHYSICAL PARAMETERS

Instrument	Satellite	Type of Measurement	Range
Electron Spectrometer	OV1-2	Electron flux, energy spectrums, and angular distribution	0.5 to 5.0 MeV in eight channels
Proton Spectrometer	OV1-2	Proton flux, energy spectrums, angular distribution	49 to 120 MeV in four channels
Proton Spectrometer	OV1-2	Integral proton flux between limits, angular distribution	1-20 MeV and 20-49 MeV
Omnidirectional Proton/Electron Spectromeners	OV1-2	Integral proton flux between limits	6-20, 40-80, 100-150 and greater than 100 MeV
	OV3-4		15-30, 30-55, 55-105, 105-170 and greater than 170 MeV
	OV1-2	Integral electron flux between limits	Greater than 0.3 and greater than 4.5 MeV
Charged Particle Spectrometer	OV3-4	Proton flux, energy spectrums, angular distribution	10.5 to 320 MeV in nine channels and greater than 320 MeV
		Electron flux, energy spectrums, angular distribution	0.5 to 4.8 MeV in six channels and greater than 4.8 MeV
		Heavy Particle flux, energy spectrums, angular distribution	11-300 MeV/nucleon in four channels

TABLE 2

TYPICAL INSTRUMENTATION FOR MEASUREMENT
of
RADIOLOGICAL PARAMETERS

Instrument	Satellite	Type of Measurement	Dynamic Range
Proton Dosimeter	OV1-2	Energy deposition at known depths in simple geometries	0.5 to 2 x 10^4 MeV/sec (each detector)
X-ray/Bremsstrahlung Dosimeter	OV1-2	Energy deposition from bremsstrahlung production in known shields	1.62 x 10^2 to 1.62 x 10^6 MeV per second
Tissue Equivalent ionization chamber (Tissue Equivalent shield material)	OV1-2	Absorbed dose in rads/hr at depths of 0.8, 3.2 and 8.0 gm/cm^2	0.2 to 200 Rad/hr
	OV3-4	Depths of 0.7, 2.9 and 4.7 gm/cm^2	10^{-2} to 10^3 Rad/hr
Tissue equivalent ionization chamber (Elemental shield)	OV3-4	Absorbed dose in rads/hr at depths: 0.2 gm/cm^2 Al	10^{-2} to 10^3 rad/hr
			10^{-4} to 10 rad/hr
		4.5 gm/cm^2 brass	10^{-3} to 10^2 rad/hr
LET Spectrometer	OV3-4	Linear Energy transfer at depths of 2.5 and 5.0 gm/cm^2	8 to 300 KeV/micron in 16 log channels

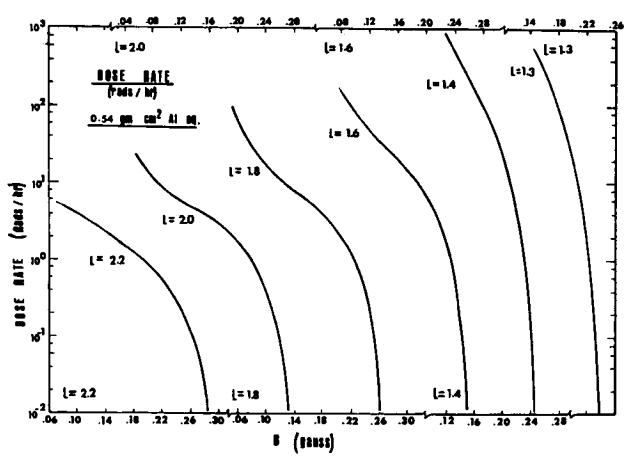

Figure 3. Typical Iso-L dose-rate profile map. The dose-rates are given in terms of amount (0.54 gm/cm^2) of aluminum equivalent material.

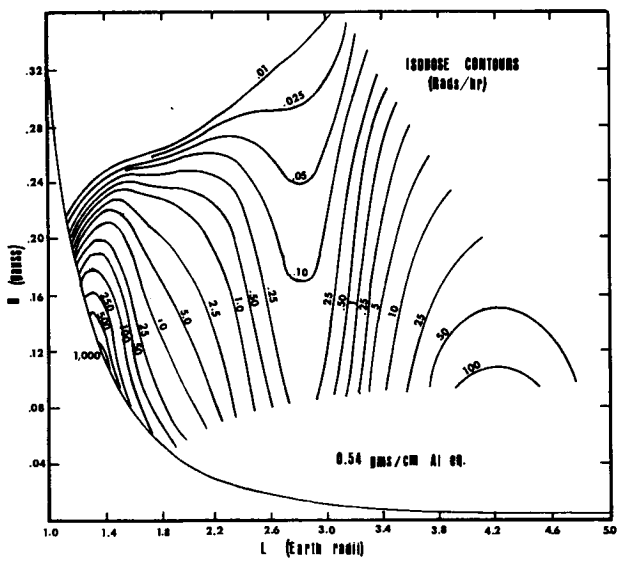

Figure 4. Typical Isodose-Rate profile map. The dose-rates are given in terms of amount (0.54 gm/cm^2) of aluminum equivalent material.

TABLE 3

DOSE-RATE MAPS PRESENTLY AVAILABLE

Shielding (gm/cm^2 Al)	Range of B (gauss)	Range of L (Earth radii)	Dose-rate Range (Rad/hr)
0.4	0.12-0.28	1.2 - 2.0	10^{-2} - 10^{2}
0.5	0.06-0.36	1.2 - 5.0	10^{-2} - 10^{3}
1.0	0.20-0.26	1.2 - 1.5	10^{-4} - 10^{0}
1.35	0.06-0.36	1.2 - 5.0	10^{-2} - 50
1.40	0.12-0.28	1.2 - 2.0	10^{-2} - 10^{2}
1.50	0.16-0.30	1.2 - 2.0	10^{-4} - 10^{1}
2.8	0.06-0.30	1.0 - 2.6	10^{-2} - 10^{1}
3.4	0.12-0.28	1.2 - 2.0	10^{-2} - 10^{1}
4.0	0.14-0.23	1.2 - 2.0	10^{-2} - 10^{1}
4.15	0.06-0.36	1.2 - 2.2	10^{-2} - 10^{3}
4.9	0.06-0.30	1.0 - 2.6	10^{-2} - 10^{1}
16.0	0.16-0.26	1.2 - 1.7	10^{-2} - 10^{1}

COMPARISON OF DOSE-RATE MEASUREMENTS WITH CALCULATIONS BASED ON PHYSICAL PARAMETERS

In those cases where extensive computer calculations using physical parameters must be performed, it is necessary to estimate the accuracy of the techniques. In order to better understand uncertainties in the transport calculations and the reliability of the available physical parameters, data from four satellites and two Gemini flights were extensively analyzed (refs. 12, 16, 19, 20, 31, 32). Data from three of the satellites included simultaneous measurements of both physical and radiological parameters and, thus, could be used to check both transport calculations per se, and dose calculations which were based on previously available data (refs 12, 17, 18). It was determined that the available physical environment was inadequate, in many cases, to accurately predict the dose-rates which were encountered. The use of simultaneously measured flux, spectrums, etc. yielded much better agreement. These data were then used to "update" the available maps and, as a check, dose-rate calculations were performed for the remaining satellite and the two Gemini flights.

The results of calculations using both the old and new environments, shown in Figure 5 and Table 4, indicate that calculations based on the old (Vette) environment underestimated the dose-rate in heavily shielded detectors where high energy (E > 80 MeV) protons contribute heavily to the dose-rate.

It was also determined (refs. 16, 31, 32) that to correctly evaluate the results of lightly shielded detectors, which are either omni-directional or do not provide "active collimation", a very sophisticated knowledge of the surrounding shielding (satellite and instrumentation) is necessary to adequately understand the data. This was also largely due to the much greater fluxes of high energy protons than had originally been estimated.

SUMMARY

Although nearly thirteen years has elapsed since the discovery of the trapped radiation environment and thousands of experiments performed, the data are insufficiently understood to accurately make estimates of radiological hazards.

Accurate calculations of doses have been possible only where precise determinations of the physical environment and spacecraft shielding were made. The only calculated results for a manned flight which were accurate to a factor of 2 were obtained using a simultaneously measured environment. In an unmanned craft on which a 1280 solid angle sectoring analysis of the shielding about the dose point was performed, the calculated and measured doses usually agreed to 50%. This latter used the new proton environment of contributions from protons with energies greater than 170 MeV.

The data from both manned and unmanned spacecraft show that the largest uncertainty is consistently in the knowledge of the radiation environment. The inner trapped region (L = 1 to 2.0) was divided into a high B and a low B region for comparison of calculation and measurement and very poor agreement was sometime found at the high magnetic field regions of the L shells, regardless of the generation of the environment used. At low magnetic field regions of the L shells, the Vette environment consistently underestimated the dose-rate by as much as a factor of 7; and the new environment, while better, yielded only a factor of 2 agreement in some regions.

The areas where manned flights occur are areas where the environmental data are most insufficient and the B-L coordinate system tends to fail. There is clearly a need for further definitions of environmental parameters.

TABLE 4

AVERAGE RATIOS OF CALCULATED TO MEASURED DOSE-RATES
for
CALCULATIONS USING THE VETTE
and
THEDE PROTON ENVIRONMENTS*

Instrument shielding (gm/cm^2 Al)	L (Earth-Radii)	Vette Environment Ratios	Thede Environment Ratios	Threshold Energy above which 50% of the dose is contirbuted (MeV)
1.4	1.3	0.48	0.48	64
	1.4	0.88	0.92	
	1.6	0.91	0.93	
	1.8	0.83	0.75	
	2.0	1.08	0.70	
3.4	1.3	0.24	0.61	94
	1.4	0.31	0.68	
	1.6	0.35	0.69	
	1.8	0.39	0.77	
	2.0	0.21	0.75	
4.0	1.2	0.25	0.63	152
	1.3	0.28	0.74	
	1.4	0.36	0.81	
	1.5	0.33	0.91	
	1.6	0.36	0.99	
	1.7	0.39	1.11	
16	1.2	0.31	0.70	190
	1.3	0.29	0.83	
	1.4	0.29	0.84	
	1.5	0.28	1.00	
	1.6	0.31	1.11	
	1.7	0.24	1.27	

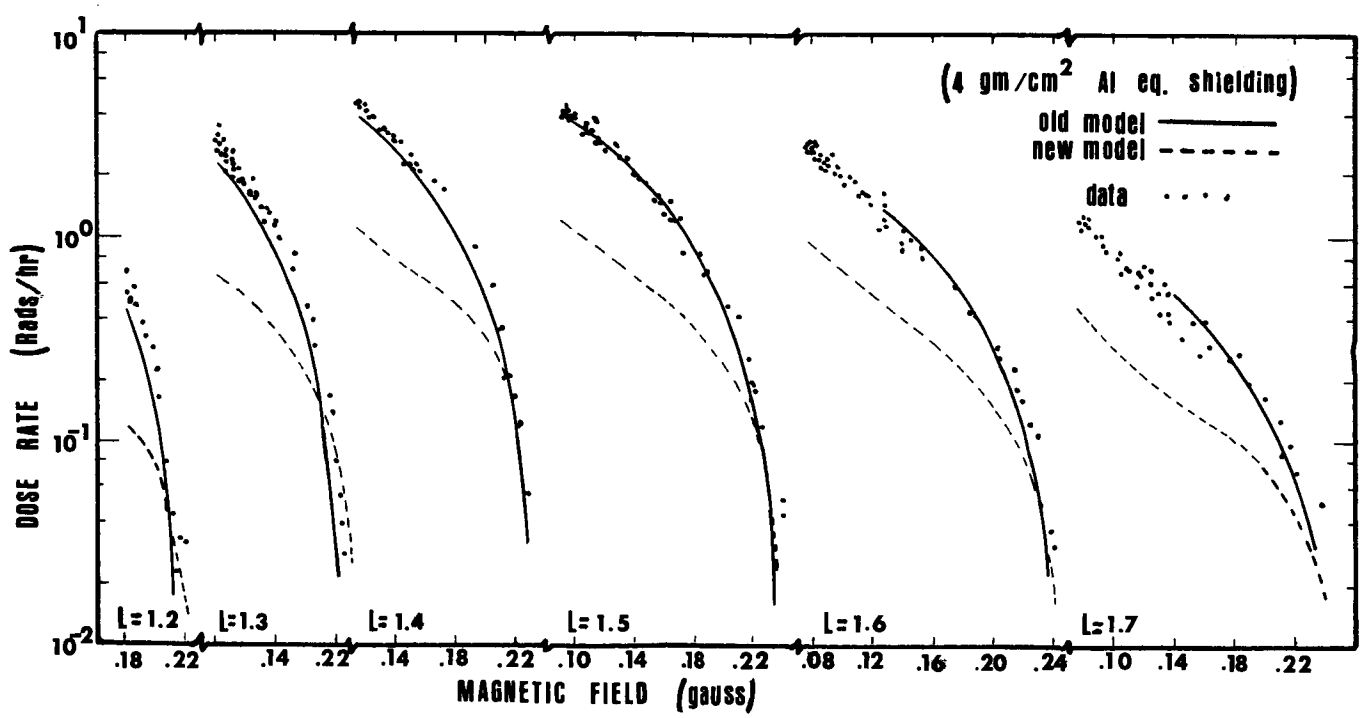

5. Iso-L dose-rate profile map for a highly shielded dose point, showing coorelation between actual measurements and calculations using both the Vette and Thede environmental models.

REFERENCES

1. Van Allen, J.A., et. al., Observation of High Intensity Radiation by Satellites 1958 Alpha and Gamma, Jet Propulsion, 28: 588-592 (1958)

2. Hess, W.N., The Radiation Belts and Magnetosphere, Bliesdell Publishing Co., Waltham, Mass. (1968).

3. Donop, W.A., Jr., Ed., TRW Space Log, Vol. 9, No. 4; TRW Systems Group, TRW Inc: (Winter 69-70).

4. Williams, D. R., Space Measurements Survey For DASA, Part II, DASA 1277, WEB No. 07.013: (Feb 65).

5. Richter, H. L., Jr., Ed., Space Measurements Survey - Instruments and Spacecraft, NASA SP-3028, T.I.D. NASA: (1966).

6. Freden, S.C. and R. S. White, Protons In the Earth's Magnetic Field, Phys. Rev. Letters, 3: 9-10 (1959).

7. Holly, F. E., et. al., Radiation Measurements to 1500 Kilometers Altitude at Equatorial Latitudes, J. Geophys. Res., 66: 1627-1639 (1961).

8. White, R. S., The Earth's Radiation Belts, Physics Today, 19: 25-38 (1966).

9. Sharp, R. D., et. al., Satellite Measurements of Low-Energy Electrons in the Northern Auroral Zones, J. Geophys. Res., 69: 2721-2730 (1964).

10. O'Brien, B. J., Review of Studies of Trapped Radiation with Satellite Bourne Apparatus, In: Space Science Reviews (C. DeJager, Ed.), D. Reidel Publishing Company, Doldrecht, Holland:415-418 (1962).

11. Shabansky, V. P., and Skuriden, G. A., Concerning the Orgin of the Earth's Radiation Belts, Foreign Translation MT-64-346.

12. McCormac, B., (Ed.), Radiation Trapped in the Earth's Magnetic Field, D. Reidel Publishing Company, Doldrecht, Holland (1966).

13. McIllwain, C. E., The Radiation Belts, Natural and Artificial, Science,142: 355-361 (1963).

14. Fillius, R. W., Trapped Protons of the Inner Radiation Belt, J. Geophys. Res., 71: 97-123 (1966).

15. Attix, F. H., and E. Tochlin, Radiation Dosimetry, Vol III, Chap. 26: 453-510, Academic Press, N.Y. (1969).

16. Holly, F. E. and J. Janni, Eds., The Current Approach to the Radiological Problems of Spaceflight, Aerospace Med., 40, 12, Sec II: 1439-1567 (Dec 1969).

17. Vette, J. I., Models of the Trapped Radiation Environment, Vol. I: Inner Zone Protons and Electrons. Vol II: Inner and Outer Zone Electrons. Vol IV: Low Energy Protons. NASA Sci. Tech. Inform. Div (1967).

18. Vette, James I., A Model Proton Environment above 4 MeV, in Radiation Trapped in the Earth's Magnetic Field, Ed. by B.M. McCormac, D. Reidel, 1966.

19. Thede, A. L., and G. E. Radke, A Correlation of Dosimetric Measurements with Charged Particle Environment of the Inner Van Allen Belt, presented at 13th Annual Meeting of the American Nuclear Society, San Diego, Calif (June 1967).

20. Thede, A.L., OV3-4 Dose Rate and Proton Spectral Measurements, AFWL-TR-68-128, Air Force Weapons Laboratory, KAFB, NM (June 1969).

21. McIllwain, C. E., Coordinates for Mapping the Distribution of Magnetically Trapped Particles, J. Geophys. Res., 66: 3681-3691 (1961).

22. Cladis, J.B., et. al., Energy Spectrum and Argular Distributions of Electrons Trapped in the Geomagnetic Fields, J. Geophys. Res., 66: 2297-2312 (1961).

23. West, H. I., et. al., Some Electron Spectra in the Radiation Belts in the Fall of 1962, Space Research V, North Holland Publ. Co., Amsterdam: 423-445 (1965).

24. Vampola, A. L. Private Communications (1967).

25. Krimigis, S. M., and Van Allen, J. A., Geomagnetically Trapped Alpha Particles, J. Geophys. Res., 72: 5779-5797 (1967).

26. Clark, B. C. Directional Sensitivity and Energy Dependance of the Gemini Dosimetry System, AFWL-TR-66-29, Air Force Weapons Laboratory KAFB, NM (May 1966).

27. Schneider, M. F., The Radiation Response of Tissue Equivalent Dosimetry Systems to 60 MeV Proton Beams, AFWL-TR-66-30, Air Force Weapons Laboratory, KAFB, NM (March 69).

28. Chapman, M. C., and Holly, F. E., An Experiment to Measure the Tissue-Equivalent Absorbed Dose (LET) and Depth-Dose Distributions Produced by Radiations in Space, In: Proceedings of the First International Congress of the International Radiation Protection Association. (W. Synder, Ed.), Pergamon Press, New York; 881-897 (1968).

29. Chapman, M. C., et. al., Development of a Cellular Absorbed Dose Spectrometer, AFWL-TR-69-76, Air Force Weapons Laboratory, KAFB, NM (Dec 1969).

30. Holly, F. E., et. Al., Results of a Space Dosimetry Experiment to Assess the Radiation Protection Calculations for Manned Space Flight, In: Proceedings of the First International Congress of Radiation Protection, Part 2 (S.S. Snyder, Ed.), Pergamon Press: 871-893 (1968).

31. Chapman, M. C., et. al., Phase I Analysis of Data Returned by the FESS Experiment from the OV1-2 Spacecraft, AFWL-TR-66-94, Air Force Weapons Laboratory, KAFB, NM (1967).

32. Fortney, R. E., Flight Experiment Shielding Study (FESS) Satellite Data Analysis - Phase II, AFWL-TR-68-108, Air Force Weapons Laboratory, KAFB, NM (Apr 1969).

33. Janni, J., Measurements of Spacecraft Cabin Radiation Distributions for the Fourth and Sicth Gemini Flights, AFWL-TR-65-149, Air Force Weapons Laboratory, KAFB, NM (Mar 67).

34. Schneider, M. F., et. al., An Active Dosimeter System to Measure Energy Deposition and Charged Particle Spectra of High Energy Inner Van Allen Belt, Solar Flare, and Galactic Cosmic Protons on Manned Spacecraft, AFWL-TR-70-29, Air Force Weapons Laboratory, KAFB, NM (Aug 70).

35. Schneider, M. F., Private Communication.